SDC

OPEN

MACULAR ATROPHY AND PHENOTYPIC VARIABILITY IN AUTOSOMAL DOMINANT STARGARDT-LIKE MACULAR DYSTROPHY DUE TO *PROM1* MUTATION

AARON M. RICCA, MD,* IAN C. HAN, MD,*† JEREMY HOFFMANN, BS,† EDWIN M. STONE, MD, PHD,*† ELLIOTT H. SOHN, MD*†

Purpose: To describe the phenotypic variability and rates of progression of atrophy in patients with *PROM1*-associated macular dystrophy.

Methods: Patients in this retrospective, longitudinal case series from a tertiary center had clinical examination and multimodal imaging performed. Areas of retinal pigment epithelium and ellipsoid zone loss over time by optical coherence tomography were calculated by two independent graders.

Results: Fifteen patients from five kindreds with an Arg373Cys mutation in *PROM1* were studied. The average age was 39 years, and 80% were women. The visual acuity was 20/40 at presentation and 20/57 at last follow-up (average 4.8 years). Three distinct macular phenotypes were observed: 1) central geographic atrophy (13%), 2) multifocal geographic atrophy (20%), and 3) bull's eye maculopathy (67%). The overall rate of atrophy progression was 0.36 mm^2/year, but the average rate of atrophy progression varied by macular phenotype: 1.08 mm^2/year for central geographic atrophy, 0.53 mm^2/year for multifocal geographic atrophy, and 0.23 mm^2/year for bull's eye maculopathy.

Conclusion: Patients with *PROM1*-associated macular dystrophy demonstrate distinct phenotypes, with bull's eye maculopathy being the most common. The average rate of atrophy progression may be similar to reported rates for *ABCA4*-related Stargardt disease and less than age-related macular degeneration. These results provide important measures for following treatment response in future gene and stem cell–based therapies.

RETINA 43:1165–1173, 2023

Autosomal dominant Stargardt-like macular dystrophy is a rare, progressive, early-onset retinal disease with high penetrance and variable phenotypic presentation. Similar to the autosomal recessive Stargardt disease due to biallelic mutations in *ABCA4*, the age of onset is typically reported between childhood to adolescence, with fundus findings that include retinal pigment epithelium (RPE) mottling and fundus flecks that can progress to a bull's eye maculopathy (BEM) or macular geographic atrophy (GA).[1–3] Initial linkage analysis for autosomal dominant Stargardt-like macular dystrophy mapped the disease to chromosome 6q,[1] and subsequent studies identified mutations in *ELOVL4*, which encodes a protein involved with membrane-bound fatty acid chain elongation.[4]

In 2010, three independent families from the Caribbean, the United Kingdom, and Italy and with an autosomal dominant inheritance pattern and Stargardt-like BEM were found to have a C to T nucleotide substitution resulting in an amino acid change of arginine to cysteine at codon 373 in the prominin-1 (*PROM1*) gene on chromosome 4.[3] The PROM1 protein is a 5-transmembrane domain protein involved in regulating fusion in photoreceptor disk morphogenesis[5,6] and has also been shown to regulate autophagy in RPE cells.[7] Several common findings reported among those affected include BEM, rod greater than cone photoreceptor dysfunction on electroretinogram (ERG), outer retinal degeneration on optical coherence tomography (OCT), progressive GA, and a hyperautofluorescent parafoveal macular

ring on fundus autofluorescence.[3] Patients can lose vision early or late in life, and there are phenotypic similarities to the advanced atrophic form of age-related macular degeneration (AMD).[8–10]

Currently, there are few longitudinal reports of patients with autosomal dominant, *PROM1*-associated macular dystrophy (PAMD),[3,11] and none documenting rates of progression of macular atrophy. The natural history of this disease is important because 1) treatments for RPE replacement and genetically corrected photoreceptor transplantation for inherited retinal diseases such as this are being developed for human trials,[12,13] 2) PAMD is an attractive disease target because it is less heterogeneous than AMD, and 3) accurate counseling for patients and their offspring is desirable.

In this study, we sought to characterize a cohort of patients with autosomal dominant Stargardt-like macular dystrophy secondary to a p.R373C mutation in the *PROM1* gene and describe longitudinal changes on multimodal imaging. We identify three primary phenotypic patterns of macular disease (BEM, multifocal GA, and central [fovea]-involving GA) and characterize the rates of atrophy progression in each phenotype.

Methods

The study protocol was approved by the Institutional Review Board for Human Subjects Research at the University of Iowa, and the study adhered to the tenets set forth in the Declaration of Helsinki. A retrospective medical record review of all patients with autosomal dominant Stargardt-like macular dystrophy due to a p.R373C mutation in the *PROM1* gene seen at the University of Iowa was performed. Detailed pedigrees were assembled, and symptomatic family members were offered clinical evaluation and genetic testing. Sanger sequencing of DNA extracted from blood samples was used to identify or confirm a p.R373C variant in *PROM1*. For the large family A in Figure 1, the mutation was initially found with next-generation sequencing after testing of multiple genes causing macular dystrophies, including *ABCA4*, *BEST1*, and *PRPH2/RDS*, were negative.

Records from all members of the families, affected or unaffected, were analyzed after coding to deidentify the protected health information. Not all examined family members were affected, and not all affected family members were alive or available for examination. Data collected were obtained as part of routine clinical care and such, and the data analyzed were variable among patients. Common data reviewed for all patients included age, sex, best-corrected visual acuity (BCVA), slitlamp biomicroscopy, dilated funduscopic evaluation, and photography. Further evaluation with Goldmann visual fields, Humphrey visual fields, fundus autofluorescence imaging, spectral domain OCT, OCT angiography, ERG, color vision testing, and flicker fusion testing were obtained when clinically applicable and available.

For patients with longitudinal OCT imaging for 12 months or more, *en face* near infrared reflectance images obtained with a confocal scanning laser ophthalmoscope (SLO) were used to quantify areas of GA (i.e., neurosensory retina and RPE atrophy) and the rate of progression over time, as previously described.[14,15] Using the region finder tool on Heidelberg Eye Explorer software (version 6.3.2.0), the atrophic regions were manually outlined for each eye at each visit, and the software calculated the outlined area in square millimeters. Areas of atrophy were outlined differently based on three different phenotypes. For eyes with a single area of GA centered on the fovea (central GA), the area of neurosensory retina and RPE atrophy was manually delineated on the SLO *en face* image. Eyes with noncontiguous areas of GA (multifocal GA) underwent manual delineation of each individual area of retina/RPE atrophy, and these areas were summed to give the total area of GA. In eyes with BEM (EZ atrophy in an annulus surrounding and sparing the fovea), no clear zone of RPE atrophy was visualized on the *en face* SLO images. In these cases, we measured the area of EZ loss because the rate of RPE and EZ loss has been reported to be similar in patients with Stargardt disease.[16] Measurements were performed twice per image for each time point by two independent graders (I.C.H. and A.M.R.; see **Figure**, **Supplemental Digital Content 1**, http://links.lww.com/IAE/B941, which shows examples of graded images). Measurements from each time point were then averaged, and the rate of atrophy was calculated in square millimeters per year for each patient eye. Average rates of atrophy progression were then calculated overall and for each separate phenotype.

From the *Department of Ophthalmology and Visual Sciences, University of Iowa Hospitals and Clinics, Iowa City, Iowa; and †Institute for Vision Research, University of Iowa, Iowa City, Iowa.

Supported by P30 EY025580 and R01 EY026547. The sponsor or funding organization had no role in the design or conduct of this research.

None of the authors has any financial/conflicting interests to disclose.

Supplemental digital content is available for this article. Direct URL citations appear in the printed text and are provided in the HTML and PDF versions of this article on the journal's Web site (www.retinajournal.com).

Reprint requests: Elliott H. Sohn, MD, Department of Ophthalmology and Visual Sciences, University of Iowa, 200 Hawkins Dr, Iowa City, IA 52242; e-mail: Elliott.sohn@gmail.com

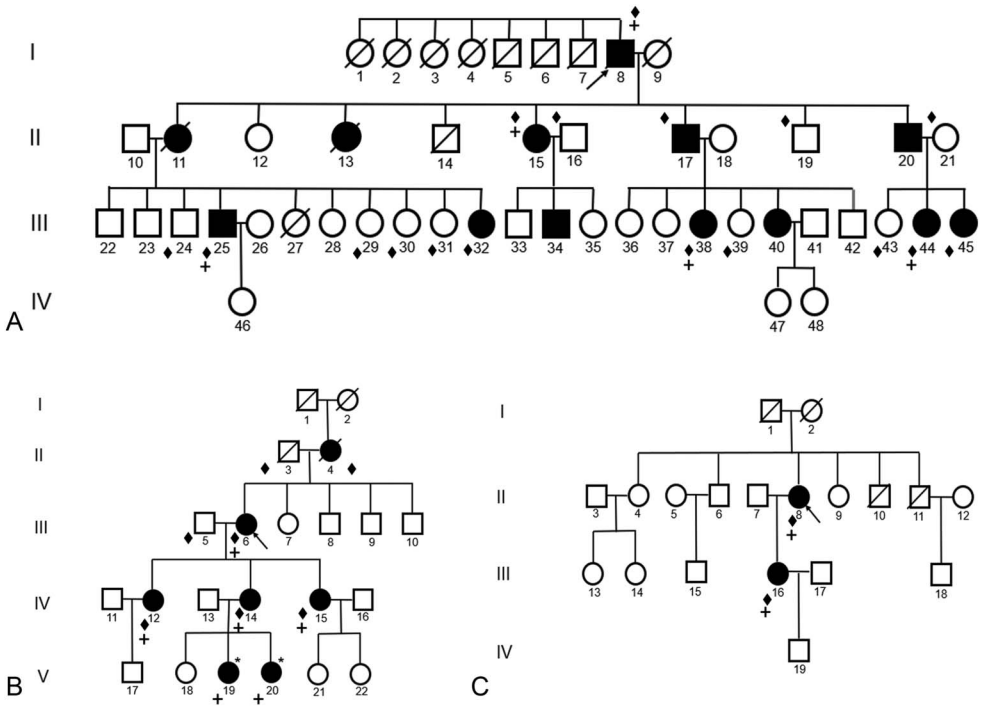

Fig. 1. A. Pedigree A shows a 48-member family with *PROM1* mutation causing macular dystrophy, of which 5 members were included in this study. **B.** Pedigree B shows a 22-member family, of which 6 patients were included in this study. **C.** Pedigree C shows a 19-member family, of which two patients were included in this study. The arrows indicate the probands, solid symbols indicate affected individuals, and the diagonal lines through the symbols indicate deceased individuals. Asterisk "*" indicates minors with phenotypic disease but no molecular confirmation; plus "+" indicates that they were studied clinically; diamond "♦" indicates that they were studied molecularly.

Results

Three families were studied (Figure 1). Family A has a 48-member pedigree. Eighteen of these 48 family members had DNA submitted for molecular studies: eight affected and 10 unaffected. In addition, five of the affected family members were examined at the University of Iowa and three were affected by report from other family members. Therefore, five patients from the 48-member family of German descent (Figure 1, Pedigree A), six patients from another single-family pedigree (Figure 1, Pedigree B), two patients were mother–daughter in an additional single-family (Pedigree C), and the remaining two patients were individuals not related to any other patients in this study, resulting in 15 patients (3 men and 12 women) who met the inclusion criteria for clinical phenotyping for this study. Molecular confirmation of a p.R373C mutation in *PROM1* was performed for all patients, with the exception of two minors (patients B:V, 19 and B:V, 20), for whom testing was deferred in the context of multiple molecularly confirmed family members (Pedigree B) and a phenotype consistent with the disease (Table 1). There was perfect segregation of the p.R373C *PROM1* variant with the macular phenotype.

The average age of included patients was 39 years (range, 9–82). Most patients initially became symptomatic in the third decade of life (range, third to fifth) with the most common initial subjective complaint being a relative central scotoma and/or decreased visual acuity. The average presenting VA was 20/40 (range, 20/15–20/320), and the average final VA was 20/57 (range, 20/15–20/1400). In contrast to *ABCA4*-associated Stargardt macular dystrophy, only 13% of patients demonstrated yellow flecks of any shape (n = 2), whereas 73% of patients were found to have nummular or bone-spicule–like pigmentation at some point through their disease course. Vascular attenuation was visualized in three patients (Table 1); one of whom, patient 15, also demonstrated a BEM with diffuse bone-spicule–like pigmentation and mild nasal VF constriction. When analyzing the refractive error, 60% of eyes (n = 18) were myopic, 20% were hyperopic (n = 6), and 6.7% were emmetropic (n = 2); data were not available for 13% (n = 4).

On funduscopic examination, three main patterns of macular atrophy were identified: central GA, multifocal GA, and BEM. Three patients, all from the single family outlined in Pedigree A, with longitudinal imaging are presented in detail below to highlight the three main patterns of macular atrophy noted in this cohort (Figures 2–4). Fundus findings for all patients revealed 10 patients with BEM (67%), three patients with multifocal GA (20%), and two patients with central GA (13%). Throughout the period of available follow-up, one patient with BEM, patient B:III, 6 went on to develop multifocal areas of GA within the parafoveal ring of atrophy that did not

Table 1. Clinical Data From Initial Presentation and Long-Term Follow-Up of Patients With *PROM1* Mutation

		Initial Examination		Final Examination					
	Sex	Age	BCVA	Age	BCVA	Type of Atrophy	Yellow Flecks	Peripheral Pigment Clumping	Vascular Attenuation
Patient A:I, 8	Male	82	20/200 OD 20/200 OS	Same	Same	Central GA	No	Yes	No
Patient A:II, 15	Female	58	20/50 OD 20/80 OS	63	20/80+1 OD 20/100 OS	Central GA	Yes	Yes	Yes
Patient A:III, 25	Male	49	20/25–1 OD 20/25–2 OS	50	20/30 OD 20/20–1 OS	BEM	No	No	No
Patient A:III, 38	Female	46	20/60+2 OD 20/320 OS	51	20/100–2 OD 10/300 OS	Multifocal GA	No	Yes	Yes
Patient A:II, 20	Male	25	20/30–2 OD 20/70 OS	37	20/1400 OD 20/1400 OS	Multifocal GA	No	Yes	No
Patient B:IV, 12	Female	24	20/20 OD 20/125 OS	34	20/100–2 OD 20/100–2 OS	BEM	No	Yes	No
Patient B:IV, 15	Female	31	20/15 OD 20/15 OS	34	20/20+2 OD 20/15–3 OS	BEM	No	No	No
Patient B:IV, 14	Female	26	20/60–2 OD 20/60–1 OS	37	20/100 OD 20/100 OS	BEM	No	Yes	No
Patient B:III, 6	Female	49	20/40–2 OD 20/20–1 OS	58	20/40–2 OD 20/40–1 OS	BEM	No	Yes	No
Patient B:V, 19	Female	10	20/20 OD 20/20+2 OS	11	20/20 OD 20/20+OS	BEM	No	No	No
Patient B:V, 20	Female	9	20/20 OD 20/20 OS	10	20/20 OD 20/20 OS	BEM	No	No	No
Patient C:III, 16	Female	32	20/20–1 OD 20/25–1 OS	Same	Same	BEM	No	Yes	No
Patient C:II, 8	Female	56	20/25 OD 20/20 OS	63	20/25–3 OD 20/20–2 OS	BEM	Yes	Yes	No
Patient 14	Female	48	20/40 OD 20/60+2 OS	55	20/125+2 OD 20/100–2 OS	Multifocal GA	No	Yes	No
Patient 15	Female	56	20/25 OD 20/25–2 OS	Same	Same	BEM	No	Yes	Yes

When able, first and most recent visit data are presented above with the age of the patient at each visit.

significantly affect the VA. The VA decreased with age in patients with central and multifocal GA, whereas patients with BEM demonstrated largely stable VA over time (Table 1).

The average duration of follow-up was 4.8 years (range, 0–12 years). Optical coherence tomography imaging data were available for 26 eyes in total, whereas 12 eyes from six patients had OCTs separated by ≥12 months for analysis of atrophy progression. Overall, patients demonstrated an average rate of atrophy progression of 0.36 mm^2/year (SD = 0.32). The average rates of atrophy progression for the different macular phenotypes were as follows: central GA 1.08 mm^2/year (SD = 0.29), multifocal GA 0.53 mm^2/year (SD = 0.31), and BEM 0.23 mm^2/year (SD = 0.14). Hyporeflective spaces in the inner retina, most consistent with degeneration, were seen in 8% of eyes (n = 2), and no patients were noted to have choroidal neovascularization on clinical examination or OCT.

The two youngest patients in the cohort, patients B:V, 19 and B:V, 20 (Figure 2), were found to have retinal pathology before any symptoms of reduced acuity. The findings consistent with disease were most readily apparent on ancillary testing rather than fundus examination. For both patients, OCT demonstrated parafoveal ellipsoid zone disruption and outer nuclear

Fig. 2. Images from the right eye of patient A:II, 15 demonstrating enlarged central GA over time. Fundus photographs showing the right eye at presentation (**A**) and progression of atrophy after 5-year follow-up (**B**). Optical coherence tomography images at presentation (**C**) and on 5-year follow-up (**D**) show enlargement of GA with loss of the outer retinal layers.

layer thinning, while an annulus of hyperautofluorescence was visualized on fundus autofluorescence surrounding the fovea.

Case Examples

Patient A:II, 15

Patient A:II, 15 first presented to our clinic at the age of 58 years. She initially noted decreased central visual acuity in her 30s. On examination, the BCVA measured 20/50 in the right eye and 20/80 in the left eye. Dilated fundus examination showed well-circumscribed, central GA in both eyes, with faint surrounding yellow flecks, mild arteriolar attenuation, and several bone-spicule–like pigment clumps peripherally (Figure 2). Optical coherence tomography demonstrated loss of the outer retinal layers and RPE in both eyes corresponding to the GA seen on fundus examination. At a follow-up visit 5 years later, the patient reported difficulty in reading and recognizing faces with a decrease in VA to 20/80 in the right eye and 20/100 in the left eye. Dilated fundus examination showed enlargement of the area of GA in both eyes (average loss, 1.08 mm^2/year [SD = 0.29]) (Figure 2).

Patient A:III, 25

Patient A:III, 25 first presented to our clinic at the age of 49 years, having only noted decreased vision for before 1–2 years. Initial examination demonstrated a visual acuity of 20/25 in both eyes, with BEM in both eyes on fundus examination (Figure 3). Optical coherence tomography demonstrated thin epiretinal membranes and a ring of perifoveal outer retinal loss with subfoveal preservation in both eyes corresponding to the BEM seen on the *en face* reflectance images (see **Figure**, **Supplemental Digital Content 2**, http://links.lww.com/IAE/B942, showing these changes), while fundus autofluorescence highlighted the parafoveal RPE damage (Figure 3). At follow-up 1 year later, the vision and examination remained stable, and the average rate of progression of atrophy for both eyes was 0.10 mm^2/year (SD = 0.04).

Patient A:III, 38

Patient A:III, 38 presented at the age of 46 years with a 10-year history of decreased central vision, reduced color vision, and nyctalopia. On initial examination, the visual acuity measured 20/60 in the right eye and 20/320 in the left eye. Dilated funduscopic evaluation demonstrated a multifocal pattern of GA with surrounding RPE mottling and arteriolar attenuation in both eyes. Scanning laser ophthalmoscopy and OCT showed loss of the outer retinal layers with subtle areas of multifocal atrophy (Figure 4). Goldmann visual fields showed central scotomata to the V4e isopter in both eyes. At a follow-up visit 5 years later, the patient likened her vision to looking

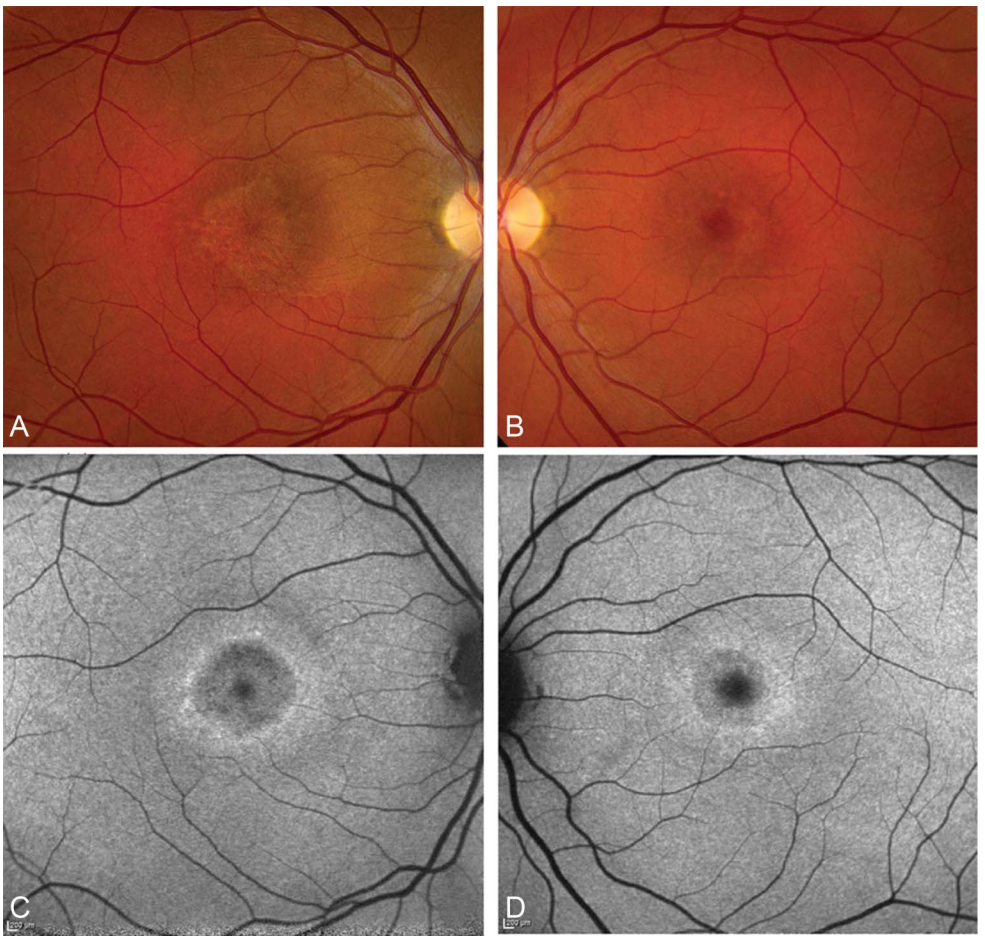

Fig. 3. Images from patient A:III, 25 demonstrating bull's eye pattern of atrophy. Fundus photographs at presentation of the right eye (**A**) and left eye (**B**) eye show BEM. Fundus autofluorescence of the right eye (**C**) and left eye (**D**) demonstrate parafoveal damaged RPE.

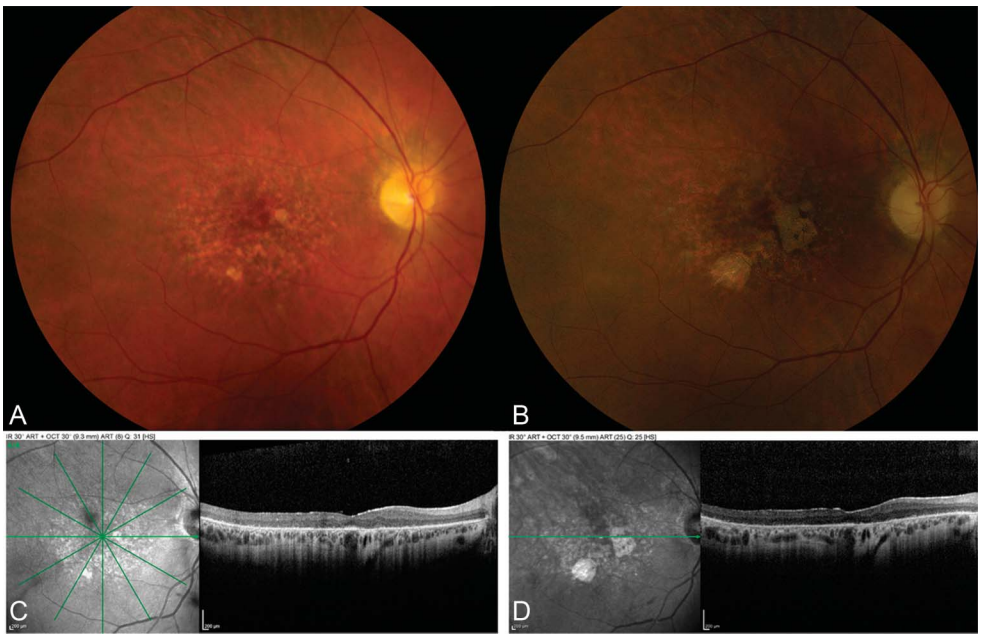

Fig. 4. Images from the right eye of patient A:III, 38 demonstrating the multifocal pattern of GA over time. Fundus photographs showing the right eye at presentation (**A**) and progression of atrophy after 5-year follow-up (**B**). Optical coherence tomography and SLO infrared images at presentation (**C**) and on 5-year follow-up (**D**) show loss of the outer retinal layers and corresponding enlargement of areas of GA.

through water and she could no longer drive or work. The VA measured 20/100 in the right eye and 10/300 in the left eye, and she was noted to have increased areas of bone-spicule–like pigmentation in the mid-periphery on dilated funduscopic evaluation. Scanning laser ophthalmoscopy and OCT demonstrated discrete areas of atrophy, increased in size relative to earlier, with corresponding enlargement of her scotomata on Goldmann visual fields. The overall average rate of atrophy progression for this patient was 0.53 mm^2/year (SD = 0.31) for the two eyes.

Discussion

Mutations in *PROM1* have been associated with a wide variety of phenotypes, ranging from predominantly macular disease resembling late-onset Stargardt macular dystrophy, to rod-predominant disease resembling retinitis pigmentosa, to early-onset severe rod-cone dystrophy along the spectrum of Leber congenital amaurosis.[3,17–23] This wide phenotypic variability is most likely related to mutation heterogeneity and modifying genes and their interplay with the differing biochemical demands between rod and cone outer segments. This study supports and elaborates on previous research by presenting longitudinal, clinical, and multimodal imaging findings from multiple pedigrees of patients with a single mutation, p.R373C variant, in *PROM1*. The patients' ages ranged from 9 to 82 years, with longitudinal follow-up spanning up to 12 years, providing insight into the natural history of this disease. The specific case examples shown highlight the wide range of phenotypic variability and the earliest findings one might expect to see. At the time of writing this article, rates of atrophy progression and ancillary imaging findings in a patient as young as 9 years have not previously been reported.

Although *PROM1*-associated autosomal dominant macular dystrophy is referred to as "Stargardt-like," our study suggests that these patients possess several key, phenotypic differences relative to classic *ABCA4*-related Stargardt disease. For example, those with *PROM1*-associated disease tended to present later in life (symptomatic in the 4th decade), relative to those with autosomal recessive Stargardt[24] disease (often symptomatic in the first and 2nd decades of life). The most common phenotype in PAMD was BEM (about two-third patients), a less common phenotype in Stargardt disease.[25] An unexpected but potentially useful finding to differentiate the two conditions is that fundus flecks, which are relatively common in classic Stargardt disease, were only present in two patients (13%) in this cohort. Along the same lines, 73% of patients developed midperipheral nummular and bone-spicule–like pigmentary changes, which is less common in *ABCA4*-associated Stargardt disease and may instead be mistaken for retinitis pigmentosa. Several patients, or affected family members, in our study were initially diagnosed with presumed autosomal dominant retinitis pigmentosa because of the strong family history and bone-spicule–like pigmentation with vascular attenuation on dilated fundus examination.

Three different families seen at our institution exhibited high penetrance and perfect segregation of the *PROM1* p.R373C variant with macular disease. There are 124,579 people who have data for this region of *PROM1* in gnomAD without a single observation of this allele, showing that p.R373C is not present in unaffected individuals in the general population. These clinical and population data strongly support the disease-causing nature of this variant and are consistent with the American College of Medical Genetics and Genomics standards and guidelines.[26]

Because of the relatively late onset of symptoms and development of GA, patients with PAMD could easily be mistaken for typical AMD, particularly in the absence of known family history. For example, several affected patients in our cohort became symptomatic in the fifth decade of life and were found to have areas of GA and as such were misdiagnosed as early-onset AMD. In patients with nonexudative AMD, those with differing patterns of macular atrophy have been reported to possess variable rates of atrophy progression.[27] Few published reports of PAMD exist, with most demonstrating a bull's eye pattern of maculopathy as the most common phenotype, and to date, there are no reports of atrophy progression in *PROM1*.[3,11] Our results suggest substantial differences in the rate of progression across different macular phenotypes. The slowest rate of progression of atrophy was seen with the BEM phenotype at an average 0.23 mm^2/year (SD = 0.14). The greatest rate of progression was seen in central GA at 1.08 mm^2/year (SD = 0.29), whereas the rate in multifocal GA was 0.53 mm^2/year (SD = 0.31). Overall, the average rate of atrophy progression was 0.36 mm^2/year (SD = 0.32) which is similar to previously reported rates of atrophy for *ABCA4*-associated Stargardt disease, which range from 0.28 mm^2/year to 1.58 mm^2/year.[28–30] By contrast, rates of GA progression in AMD range from 0.53 to 2.6 mm^2/year with a median of 1.78 mm^2/year.[31] Similarly, BCVA in those with central GA steadily decreased over time, while patients with a BEM demonstrated largely stable BCVA over time. Patients with multifocal GA demonstrated the most widely variable BCVA with some eyes maintaining excellent

acuity and others developing the worst VA in the cohort, 20/1400.

Although three distinct macular phenotypes were identified in this study, these groups are not necessarily mutually exclusive, and these phenotypes may represent stages of disease. For example, one patient who presented with BEM went on to develop multifocal GA. Thus, an understanding of the varying rates of progression between phenotypes is important when counseling the patient on prognosis and may be important to consider when measuring disease progression or treatment response in eventual therapeutic trials.

The limitations of this study include its limited sample size and its retrospective nature. Gender predilection would not be expected in an autosomal dominant inheritance pattern; however, this cohort contains a disproportionate number of female patients, which could induce an unintended gender bias in the data. Statistical analysis comparing rates of atrophy between groups was not performed because of the small sample size. Although our study provides the first estimate of atrophy size and progression in PAMD, we did not have sufficient power to evaluate the effect of other factors on progression, including age or initial lesion size. Similarly, detailed comparison of ancillary testing (e.g., ERG, Goldmann visual fields) was not performed because these data were not available for every patient. Because p.R373C mutation in *PROM1* is the only dominant variant associated with isolated macular dystrophy to our knowledge, we do not know whether similar clinical features would be seen in other mutations involving the same functional domain.

PROM1-associated autosomal dominant Stargardt-like macular dystrophy is a relatively recently recognized clinical entity. The findings presented expand on our understanding of the natural history of the disease and provide the first quantitative data on rate of atrophy progression based on longitudinal analysis, which may be useful in future therapeutic trials.

Key words: PROM1, macular dystrophy, age-related macular degeneration, Stargardt disease, AMD, ABCA4, OCT, bull's eye maculopathy, geographic atrophy.

References

1. Stone EM, Nichols BE, Kimura AE, et al. Clinical features of a Stargardt-like dominant progressive macular dystrophy with genetic linkage to chromosome 6q. Arch Ophthalmol 1994; 112:765–772.
2. Cibis GW, Morey M, Harris DJ. Dominantly inherited macular dystrophy with flecks (Stargardt). Arch Ophthalmol 1980;98: 1785–1789.
3. Michaelides M, Gaillard MC, Escher P, et al. The PROM1 mutation p.R373C causes an autosomal dominant bull's eye maculopathy associated with rod, rod-cone, and macular dystrophy. Invest Opthalmol Vis Sci 2010;51:4771–4780.
4. Agbaga MP, Brush RS, Mandal MNA, et al. Role of Stargardt-3 macular dystrophy protein (ELOVL4) in the biosynthesis of very long chain fatty acids. Proc Natl Acad Sci 2008;105: 12843–12848.
5. Yang Z, Chen Y, Lillo C, et al. Mutant prominin 1 found in patients with macular degeneration disrupts photoreceptor disk morphogenesis in mice. J Clin Invest 2008;118:2908–2916.
6. Han Z, Anderson DW, Papermaster DS. Prominin-1 localizes to the open rims of outer segment lamellae in Xenopus laevis rod and cone photoreceptors. Invest Opthalmol Vis Sci 2012; 53:361–373.
7. Bhattacharya S, Yin J, Winborn CS, et al. Prominin-1 is a novel regulator of autophagy in the human retinal pigment epithelium. Invest Opthalmol Vis Sci 2017;58:2366–2387.
8. Holz FG, Strauss EC, Schmitz-Valckenberg S, van Lookeren Campagne M. Geographic atrophy: clinical features and potential therapeutic approaches. Ophthalmology 2014;121:1079–1091.
9. Sohn EH, Flamme-Wiese MJ, Whitmore SS, et al. Choriocapillaris degeneration in geographic atrophy. Am J Pathol 2019; 189:1473–1480.
10. Whitmore SS, Sohn EH, Chirco KR, et al. Complement activation and choriocapillaris loss in early AMD: implications for pathophysiology and therapy. Prog Retin Eye Res 2015;45:1–29.
11. Palejwala NV, Gale MJ, Clark RF, et al. Insights into autosomal dominant stargardt-like macular dystrophy through multimodality diagnostic imaging. Retina 2016;36:119–130.
12. Burnight ER, Gupta M, Wiley LA, et al. Using CRISPR-cas9 to generate gene-corrected autologous iPSCs for the treatment of inherited retinal degeneration. Mol Ther 2017;25:1999–2013.
13. Scruggs BA, Jiao C, Cranston CM, et al. Optimizing donor cellular dissociation and subretinal injection parameters for stem cell-based treatments. Stem Cell Transl Med 2019;8: 797–809.
14. Domalpally A, Danis R, Agron E, et al. Evaluation of geographic atrophy from color photographs and fundus autofluorescence images: age-related eye disease study 2 report number 11. Ophthalmology 2016;123:2401–2407.
15. Reumueller A, Sacu S, Karantonis MG, et al. Semi-automated quantification of geographic atrophy with blue-light autofluorescence and spectral-domain optical coherence tomography: a comparison between the region finder and the advanced retinal pigment epithelium tool in the clinical setting. Acta Ophthalmologica 2019;97:e887–e895.
16. Cai CX, Light JG, Handa JT. Quantifying the rate of ellipsoid zone loss in stargardt disease. Am J Ophthalmol 2018;186:1–9.
17. Cehajic-Kapetanovic J, Birtel J, McClements ME, et al. Clinical and molecular characterization of PROM1-related retinal degeneration. JAMA Netw Open 2019;2:e195752
18. Lee W, Paavo M, Zernant J, et al. Modification of the PROM1 disease phenotype by a mutation in ABCA4. Ophthalmic Genet 2019;40:369–375.
19. Salles MV, Motta FL, Dias da Silva E, et al. PROM1 gene variations in Brazilian patients with macular dystrophy. Ophthalmic Genet 2017;38:39–42.
20. Del Pozo-Valero M, Martin-Merida I, Jimenez-Rolando B, et al. Expanded phenotypic spectrum of retinopathies associated with autosomal recessive and dominant mutations in PROM1. Am J Ophthalmol 2019;207:204–214.

21. Liang J, She X, Chen J, et al. Identification of novel PROM1 mutations responsible for autosomal recessive maculopathy with rod-cone dystrophy. Graefes Arch Clin Exp Ophthalmol 2019;257:619–628.
22. Permanyer J, Navarro R, Friedman J, et al. Autosomal recessive retinitis pigmentosa with early macular affectation caused by premature truncation in PROM1. Invest Opthalmol Vis Sci 2010;51:2656–2663.
23. Zhang Q, Zulfiqar F, Xiao X, et al. Severe retinitis pigmentosa mapped to 4p15 and associated with a novel mutation in the PROM1 gene. Hum Genet 2007;122:293–299.
24. Stargardt K. Über familiäre, progressive Degeneration in der Maculagegend des Auges. Albrecht von Græfe's Archiv für Ophthalmologie 1909;71:534–550.
25. Schindler EI, Nylen EL, Ko AC, et al. Deducing the pathogenic contribution of recessive ABCA4 alleles in an outbred population. Hum Mol Genet 2010;19:3693–3701.
26. Richards S, Aziz N, Bale S, et al. Standards and guidelines for the interpretation of sequence variants: a joint consensus recommendation of the American College of medical genetics and Genomics and the association for molecular pathology. Genet Med 2015;17:405–424.
27. Schmitz-Valckenberg S, Sahel JA, Danis R, et al. Natural history of geographic atrophy progression secondary to age-related macular degeneration (geographic atrophy progression study). Ophthalmology 2016;123:361–368.
28. McBain VA, Townend J, Lois N. Progression of retinal pigment epithelial atrophy in stargardt disease. Am J Ophthalmol 2012;154:146–154.
29. Testa F, Melillo P, Di Iorio V, et al. Macular function and morphologic features in juvenile stargardt disease: longitudinal study. Ophthalmology 2014;121:2399–2405.
30. Strauss RW, Munoz B, Ho A, et al. Progression of stargardt disease as determined by fundus autofluorescence in the retrospective progression of stargardt disease study (ProgStar report No. 9). JAMA Ophthalmol 2017;135:1232–1241.
31. Fleckenstein M, Mitchell P, Freund KB, et al. The progression of geographic atrophy secondary to age-related macular degeneration. Ophthalmology 2018;125:369–390.